



## Radial Velocities of Stars in Globular Clusters: a Look into $\omega$ Cen and 47 Tuc

*M. Mayor and G. Meylan, Geneva Observatory, Switzerland*

Subjected to dynamical investigations since the beginning of the century, globular clusters still provide astrophysicists with theoretical and observational problems, which so far have only been partly solved.

If for a long time the star density projected on the sky was fairly well represented by simple dynamical models, recent

photometry of several clusters reveals a cusp in the luminosity function of the central region, which could be the first evidence for collapsed cores.

The development of photoelectric cross-correlation techniques for the determination of stellar radial velocities opened the door to kinematical investigations (Gunn and Griffin, 1979,

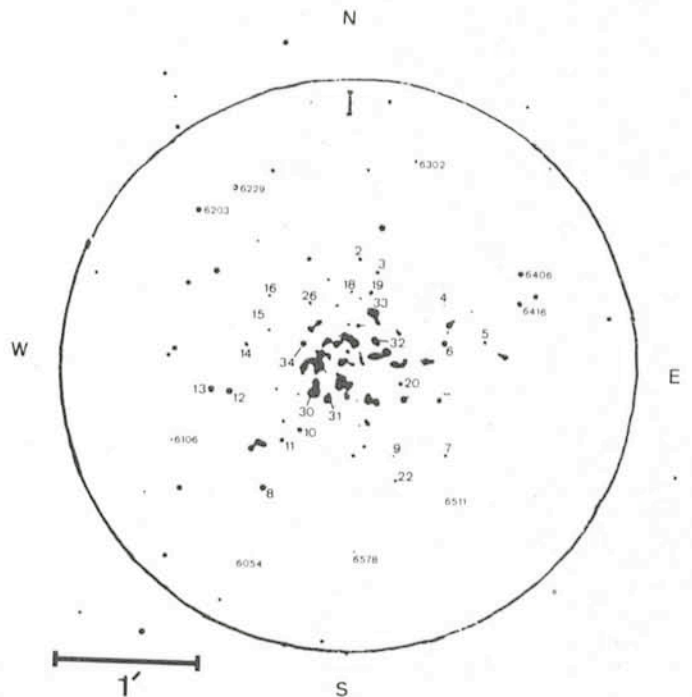
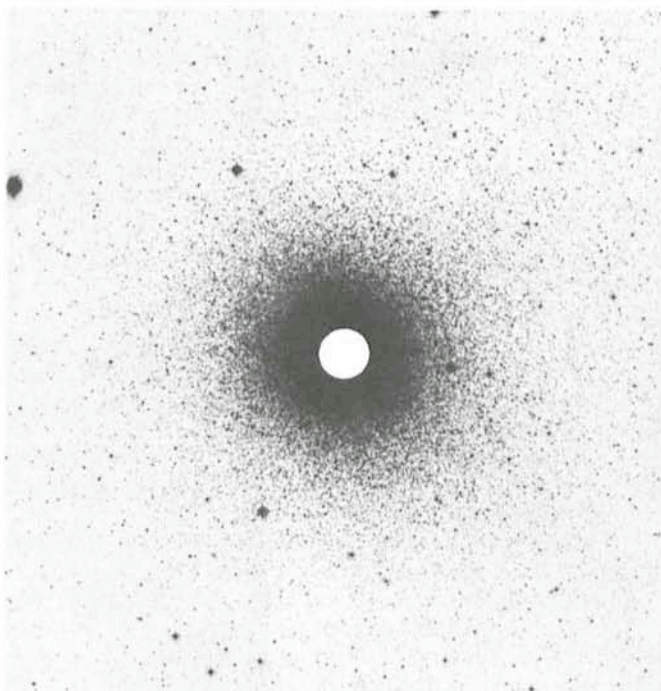


Fig. 1: Left: 47 Tuc (NGC 104) from the Deep Blue Survey – SRC-(J). Right: Centre of 47 Tuc from a near-infrared photometric study of Lloyd Evans. The diameter of the large circle corresponds to the disk of the left photograph. The maximum of the rotation appears inside the circle; the linear part of the rotation curve (solid-body rotation) affects only stars inside one arcminute of the centre.

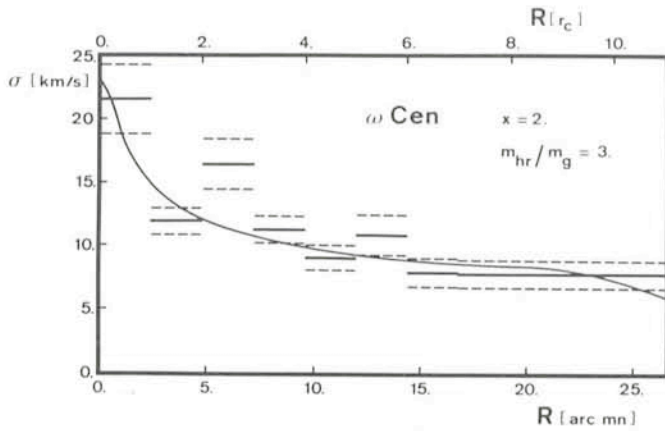


Fig. 4:  $\omega$  Cen: observed velocity dispersion and model velocity dispersion (continuous line) computed with IMF exponent  $x = 2$  and with  $m_{hr}/m_g = 3$ , where  $m_{hr}$  is the mean individual mass of heavy remnants and  $m_g$  the individual mass of a giant star.

- (iv) the differential rotation in the outer parts
- (v) the decrease of rotation towards the poles because of non-cylindrical rotation.

After subtraction of the radial component of the spatial velocity of each cluster as a whole ( $\bar{V} = 232.6$  km/s for  $\omega$  Cen;  $\bar{V} = -19.5$  km/s for 47 Tuc), the rotational velocity fields are clearly displayed.

Fig. 2 shows the equatorial rotation curve of  $\omega$  Cen whereas the non-cylindrical character of the rotation appears in Fig. 3. It is interesting to point out the structural resemblance between both clusters through the fact that the rotational velocity peaks in both cases between 3 and 4 core radii.

### Velocity Dispersion

Contributions of rotation and integration along the line of sight having been eliminated, the velocity dispersion component due only to random motions was obtained, under the assumption of isotropy, in a few concentric shells: for  $\omega$  Cen, Fig. 4 and for 47 Tuc, Fig. 5. These results show the same tendency in both clusters: a slow and regular increase of the velocity dispersion from the edge of the cluster towards the centre, with large values in the core.

In order to discuss these surprising results, it is worthwhile to recall that if Gunn and Griffin (1979) do not find this central increase in their study of M3 (NGC 5272), this is due to the fact

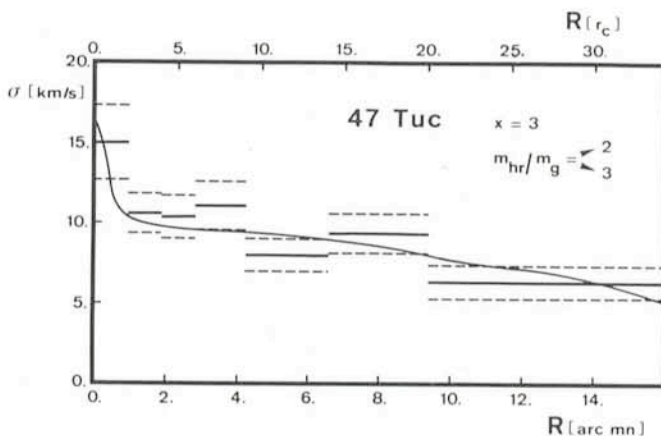


Fig. 5: 47 Tuc: observed velocity dispersion and model velocity dispersion (continuous line) computed with IMF exponent  $x = 3$  and with  $m_{hr}/m_g = 2$  and 3 (both cases give the same result).

### Tentative Time-table of Council Sessions and Committee Meetings in 1985

November 12	Scientific Technical Committee
November 13-14	Finance Committee
December 11-12	Observing Programmes Committee
December 16	Committee of Council
December 17	Council

All meetings will take place at ESO in Garching.

that they did not take into account two very-high velocity member stars of this cluster. If these two stars situated in the core of M3 are added to the sample of stars, the central velocity dispersion increases and shows a value greater than those of regions immediately outside.

For  $\omega$  Cen and 47 Tuc, the distributions of residual velocities in the different shells were investigated. They do not present any significant divergence from normal laws, nor do they have very high velocity stars. Hence the large central values of the velocity dispersions obtained in the centres of  $\omega$  Cen and 47 Tuc are not due to a few stars with exceptional velocities.

The dynamical importance of binaries in the evolution of globular clusters is now well established; in particular, because of equipartition, heavy binaries should be concentrated in the core. Thus it would be possible to think that at least a part of the central increase of the velocity dispersion could be explained by the existence of orbital motions of binary stars. The twice measured stars in the cores of  $\omega$  Cen and 47 Tuc do not seem to confirm this idea.

The relative importance of ordered and random motions are given by the ratio  $v_o/\sigma_o$ , where  $v_o^2$  is the mass-weighted mean square rotation speed and  $\sigma_o^2$  the mass-weighted mean square random velocity along the line of sight.

The results visible in Fig. 6 show that  $\omega$  Cen and 47 Tuc are in close agreement with models of oblate axisymmetric systems

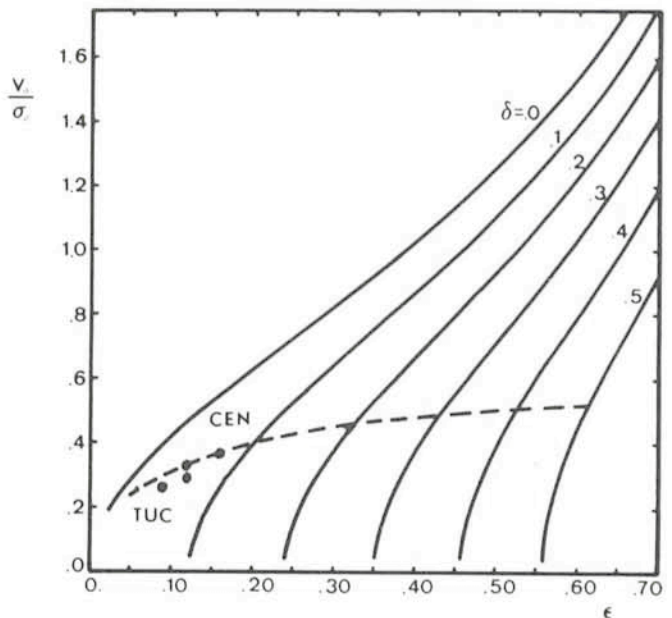


Fig. 6: Ratio  $v_o/\sigma_o$  of ordered to random motions in function of ellipticity  $\epsilon$  and anisotropy  $\delta$ . Due to the strong influence of the central part of the clusters, the present observed positions of  $\omega$  Cen and 47 Tuc are in favour of a negligible anisotropy of the velocity distribution in the few central core radii.

study of M3). Radial velocities with an accuracy better than 1 km/s (about one tenth of typical internal motions in a globular cluster) are determined despite the relative faintness of these stars. This gives access, for example, to an understanding of the behaviour of the velocity dispersion as a function of the distance to the centre, to details of the field of rotation and to a search for spectroscopic binaries.

The latter, formed by dissipative two-body tidal capture or by three-body encounters, play an essential role in the dynamical evolution of a self-gravitating system. Depending on the formation mode, binaries can give up energy to passing stars, becoming more and more tightly bound. The energy made available may slow down or even reverse the collapse of the core.

### Accurate Radial Velocities thanks to CORAVEL

Set up at the Cassegrain focus of the 1.5 m Danish telescope at La Silla, the CORAVEL photoelectric spectrometer provides high-quality radial velocities (Baranne et al. 1979, *Vistas in Astronomy*, **23**, 279).

The mean accuracy per measurement is 0.6 and 0.9 km/s for 47 Tuc and  $\omega$  Cen respectively. More than 600 radial velocity measurements of stars, mainly between B mag 13 and 15, have been carried out through collaboration between observers from ESO, the Copenhagen, Marseilles and Geneva Observatories (Mayor et al, 1983, *Astron. Astrophys. Suppl.* **54**, 495).

The kinematical and dynamical description given below was obtained through the mean radial velocities of 298 member stars in  $\omega$  Cen and 192 member stars in 47 Tuc. These stars are uniformly distributed from the centres to 9.3 core radii for  $\omega$  Cen and to 30.5 for 47 Tuc.

King's concentration parameters  $c = \log(r_t/r_c)$ , logarithm of the ratio of the tidal radius  $r_t$  to the core radius  $r_c$ , for these two clusters underline their important differences of structure:  $\omega$  Cen is a rather loose cluster with  $c = 1.36$ ,  $r_c = 2.4$  arcmin,  $r_t = 55$  arcmin, whereas 47 Tuc shows a strongly condensed core with  $c = 2.03$ ,  $r_c = 0.47$  arcmin and  $r_t = 50$  arcmin. This structural disparity involves immediate consequences on the observation of individual stars in the central regions: there is no problem of identification of stars in  $\omega$  Cen even inside one core radius but for 47 Tuc the high central brightness saturates all the photographic plates. Nevertheless, since the acquisition of very central radial velocities is essential for determining the maximum of the rotation law as well as for obtaining the

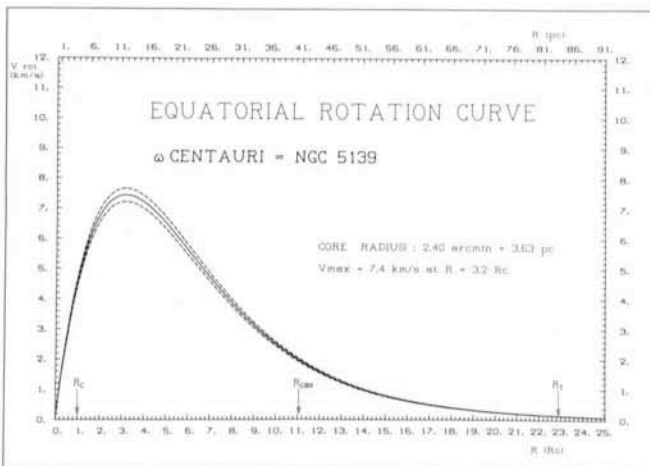


Fig. 2: Equatorial rotation curve of  $\omega$  Cen deduced from radial velocities of 298 individual stars (under the hypothesis that the cluster is viewed equator-on).

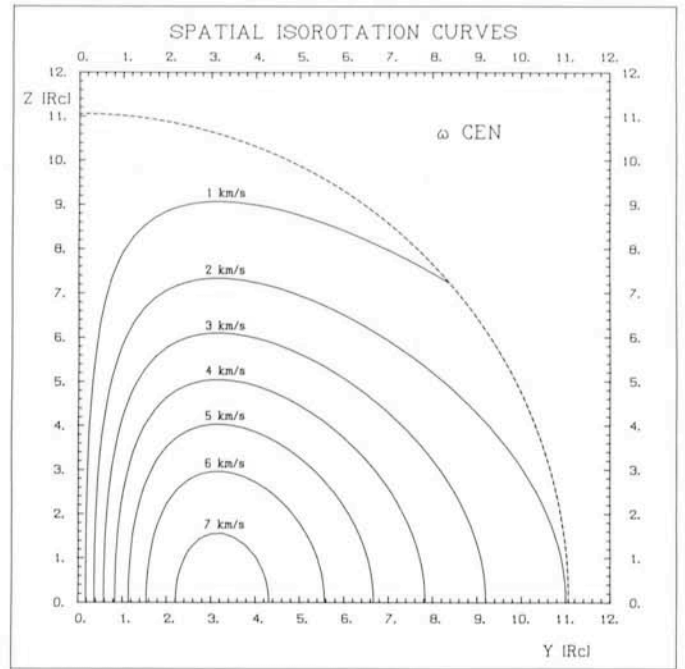


Fig. 3: Smoothed velocity field deduced from  $\omega$  Cen radial velocity measurements: spatial isorotation curves drawn on a meridional plane containing the rotation axis of the cluster (under the hypothesis of an equator-on view of the cluster)

real central velocity dispersion, an IR plate of the nucleus of 47 Tuc (Lloyd Evans, 1974) was used to identify central stars. We were extremely lucky to discover that, by decreasing the gain of the TV monitor at the 1.5 m Danish telescope, the inner part of this cluster appeared very similar to the IR chart (Fig. 1), thus making the measurement of radial velocities of individual stars feasible.

### Rotation

It is well known that the flattening of elliptical galaxies is not necessarily due only to rotation, the latter being generally too weak to explain the large observed ellipticities. An alternative to galaxian rotation seems to be an anisotropy of the velocity dispersion in triaxial ellipsoids or oblate spheroids. In the case of globular clusters, the problem looks different; we then observe the internal parts in which the relaxation time scale is relatively short. Thus, at least in the central parts where rotation is expected, velocity dispersion obtained through dynamical models of globular clusters appears nearly isotropic. Given the small mean ellipticities of these clusters, we may think that their flattening is due to rotation, the latter being generally weak and therefore detectable with difficulty. Even though the rotation of some globular clusters had already been detected ( $\omega$  Cen by Harding, ROB, 1965; M13 by Gunn and Griffin [unpublished]; 47 Tuc by Mayor et al, 1984, *AA* **134**, 118), no detailed velocity field  $V(r, z)$  was determined (distance  $r$  to the rotation axis and  $z$  to the equatorial plane).

The main characteristics of the velocity fields for the two clusters studied can be summarized as follows:

- (i) solid-body rotation in the nucleus  
 $\omega$  Cen :  $\Omega_c = 4.6 \text{ km s}^{-1} r_c^{-1} = 1.3 \cdot 10^{-6} \text{ y}^{-1}$   
 47 Tuc :  $\Omega_c = 2.7 \text{ km s}^{-1} r_c^{-1} = 4.9 \cdot 10^{-6} \text{ y}^{-1}$
- (ii) the maximum velocity  $V_{\max}$
- (iii) the position of this maximum as a function of the radius  
 $\omega$  Cen :  $V_{\max} = 7.4 \text{ km s}^{-1}$  at  $r = 3.2 r_c$   
 47 Tuc :  $V_{\max} = 4.6 \text{ km s}^{-1}$  at  $r = 3.5 r_c$

with small ellipticity and slight anisotropy. The dashed line shows the trajectory followed by  $[v_o(i)/\sigma_o, \epsilon_{app}(i)]$  when  $i$  decreases from  $90^\circ$  (equator on) while  $\epsilon_{true}$ , the true ellipticity, and  $\delta$ , the anisotropy parameter, are held constant. For both of these clusters results are given for  $i = 90^\circ$  and  $60^\circ$ .

### Masses and Mass-Luminosity Ratios

The simultaneous knowledge of the velocity dispersion  $\sigma(r) = \sqrt{v^2(r)}$  (corrected for rotation) and of the normalized space density distribution  $v(r) = \varrho(r)/\varrho(0)$  of a population of test particles (here the giant star population) moving in a spherical cluster allows, under the hypothesis of the velocity dispersion isotropy, to determine directly the total gravitational potential. In the same order of approximation, the weak rotation can here be neglected. It is then possible to deduce the total dynamical mass  $M(r)$  inside the radius  $r$  of the cluster, via the following equation:

$$\frac{GM(r)}{r} = -\sigma^2 \left[ \frac{d \ln v}{d \ln r} + \frac{d \ln \sigma^2}{d \ln r} + 2\beta \right]$$

where  $\beta = 0$  for the systems with isotropic velocity dispersion. However, in globular cluster cores, the limited number of stars for which the radial velocity can be determined does not allow a sufficiently precise determination of  $\sigma(r)$  in order to give the variations of  $d \ln \sigma^2 / d \ln r$  in the central regions. The same lack of accuracy affects the knowledge of  $d \ln v / d \ln r$ .

If we suppose on the one hand that the cluster consists of several sub-populations with different individual masses and, on the other hand, equipartition of the energy, the shape of the function  $\sigma(r)$  can be deduced. The radial variation of  $\sigma(r)$  depends on the percentage of heavy remnants (degenerated stars with masses larger than the mass of the test particles), on the mass function of the main sequence and on the total mass of the cluster. Certainly, such an approach would benefit from

a better defined luminosity function of the lower part of the main sequence (an expected task for the Space Telescope).

The observed dependence of the velocity dispersion with the distance to the centre implies, for any chosen IMF compatible with the total luminosity constraint, the presence of heavy remnants in the core of  $\omega$  Cen. These objects, with individual masses larger than the giant stars by a factor of 2 or 3, represent about 7 per cent of the total mass of the cluster. Due to mass segregation, the ratio of the density of heavy remnants to the total density is very large in the nucleus (for  $\omega$  Cen this ratio can be of about 35 %).

On the other hand, the radial velocity dispersion of 47 Tuc seems to require only 1 to 3 per cent of heavy remnants in comparison to the total mass.

For these two globular clusters, the total masses derived from our analysis are:

$$\begin{aligned} \text{total mass of } \omega \text{ Cen} &\approx 2.9 \cdot 10^6 \text{ solar masses} \\ \text{total mass of 47 Tuc} &\approx 1.3 \cdot 10^6 \text{ solar masses} \end{aligned}$$

which implies mass-to-luminosity ratios between 2 and 3.

The sub-population with individual masses between 1.5 and 2 solar masses consists most probably of the remnants issued from the evolution of the most massive stars of the globular clusters initial mass function. But part of this sub-population could also be binaries. The observed radial distribution of X-ray sources in globular clusters presents a notable concentration towards the core, in agreement with the dynamical segregation of individual masses of about 1.5 solar masses.

If the fact that the high stellar densities expected in collapsed cores are favourable to binary formation and if the detected X-ray sources are binaries, it would be important to recall the total absence (or at least large deficiency) of spectroscopic binaries in globular clusters. Continuing observations of stellar radial velocities, particularly in the cores of globular clusters, should create some new constraints regarding their dynamics.

## R136a and the Central Object in the Giant HII Region NGC 3603 Resolved by Holographic Speckle Interferometry

G. Weigelt, G. Baier and R. Ladebeck, *Physikalisches Institut Erlangen*

R136 (HD 38268) is the mysterious central object of the 30 Doradus nebula in the Large Magellanic Cloud (Walborn, 1973). R136 consists of the bright component R136a and the fainter components R136b and R136c (Feitzinger et al., 1980). There exist mainly two opinions about the nature of R136a: that it is either a supermassive object with  $M \sim 1,000$  to  $3,000 M_\odot$  (Schmidt-Kaler and Feitzinger, 1981; Cassinelli et al., 1981) or that it is a dense star cluster consisting of O and WR stars (Moffat and Seggewiss, 1983; Melnick, 1983).

Speckle interferometry observations (Labeyrie, 1970) of R136a have been reported by Weigelt (1981), Meaburn et al. (1982) and Weigelt (1984). Our speckle measurements of the  $0''.5$  component are in agreement with visual observations made by Innes (1927) and Worley (1984) as well as with photographic measurements by Chu et al. (1984) and by Walker and O'Donoghue (1985).

In this paper we show the first diffraction-limited true image of R136a (Fig. 2). This image shows that R136a is a dense star cluster consisting of at least 8 stars. It was possible to reconstruct a true image of R136a1 to a8 by using R136b (separation  $\sim 2''.1$ ) and R136c (separation  $\sim 3''.3$ ) as deconvolution keys (holographic speckle interferometry). The

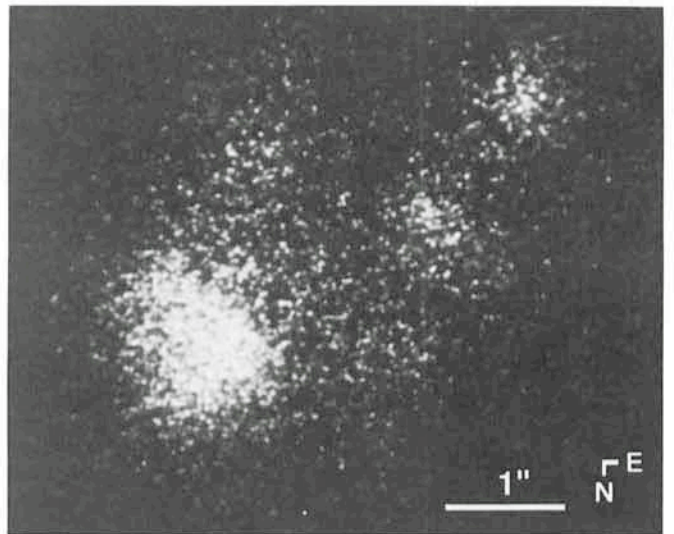


Fig. 1: Speckle interferogram of R136. The brightest speckle cloud is R136a, the other speckle clouds are R136b to e (filter RG 610, exposure time 1/15 sec).